Journal of Luminescence 203 (2018) 467–472

Contents lists available at ScienceDirect

Journal of Luminescence

journal homepage: www.elsevier.com/locate/jlumin

Suppression of metal-to-metal charge transfer quenching in Ce^{3+} and Eu^{3+} comprising garnets by core-shell structure

Stefan Fischer*, Florian Baur, Thomas Jüstel*

Department of Chemical Engineering, Münster University of Applied Sciences, Stegerwaldstraße 39, D-48565 Steinfurt, Germany

A R T I C L E I N F O

Keywords:
Core-shell materials
Metal-to-metal charge transfer quenching
Energy transfer
Phosphor converted LEDs
Photoluminescence
Rare earth garnets
Solid state lighting

A B S T R A C T

This work concerns a novel Eu^{3+} activated phosphor sensitized by Ce^{3+} in order to obtain absorption in the blue spectral range in combination with line emission in the red spectral range. It is well known that this approach suffers from metal-to-metal charge transfer (MMCT) quenching between Ce^{3+} and Eu^{3+}. To reduce this quenching mechanism in $Tb_3Al_5O_{12}$ (TAG), the sensitizer and activator were spatially separated by creating core-shell particles. Various powder samples including core-shell and non-core-shell particles were prepared via precipitation synthesis and post-annealing steps. The phase purity of the synthesized particles was determined by X-ray powder diffraction. Scanning electron microscope images have been taken to study the particle morphology and shell formation. It turned out that nearly uniform shells could be achieved by precipitation synthesis with urea as precipitant. The photoluminescence properties were investigated by recording emission spectra as well as diffuse reflectance spectra. Furthermore, temperature dependent emission spectra and fluorescence lifetimes were measured to compare thermal quenching and decay behavior of the samples. With around 60%, the external quantum efficiencies (EQE) of TAG:Ce^{3+} and TAG:Ce^{3+}@TAG:Eu^{3+} core-shell particles are almost identical. Since the EQE of non-core-shell TAG:Ce^{3+},Eu^{3+} is lower than 5%, it could be demonstrated that the core-shell approach significantly increases the EQE by spatial separation of Ce^{3+} and Eu^{3+}.

1. Introduction

Due to the high luminous efficacy (LE), long lifetime, small form factor and high wall plug efficiency, light emitting diodes (LEDs) are heading for the unrivalled contender in lighting applications [1,2]. A general restriction for further market penetration of phosphor converted light emitting diodes (pcLEDs), particularly into the indoor lighting market, is the limited amount of suitable narrow band red emitting phosphors to improve color rendering and to reduce color temperature without simultaneously reducing the LE [3]. Most of the white emitting pcLEDs exhibit a moderate color rendering index (CRI) as well as a high correlated color temperature (CCT) between 4000 and 8000 K due to a lack of red emission which leads to perception of a cool white light [4,5]. Lately, K_2SiF_6:Mn^{4+} has been introduced as a narrow band red emitting phosphor by GE. However, synthesis of this phosphor involves hydrofluoric acid and stabilization is required to prevent a redox reaction between Mn^{4+} and F^-. Therefore, finding an oxide based alternative is still of importance. There are several established red line emitting oxide phosphors, activated with Eu^{3+}, for fluorescent lamps and display applications [6]. For use in pcLEDs, such phosphors would require strong absorption in the blue spectral range, since most of the white emitting pcLEDs comprise a highly efficient blue emitting (In,Ga)N-chip [7,8]. Regrettably, Eu^{3+} activated phosphors do not show sufficient absorption in the blue spectral range and, thus, solitary application of these phosphors in combination with blue emitting LEDs is not possible [9].

An approach to avoid the above-mentioned drawback is to sensitize Eu^{3+} by a co-dopant which strongly absorbs radiation in the blue spectral range and transfers the energy to Eu^{3+} [10]. $BaMgAl_{10}O_{17}$:Eu^{2+},Mn^{2+} and $LaPO_4$:Ce^{3+},Tb^{3+} are widely established phosphors wherein co-doping with a sensitizer to achieve efficient sensitization is applied [11,12]. The sensitization of Eu^{3+} with Ce^{3+} is generally possible, since the 5d → 4f emission of Ce^{3+} overlaps with various Eu^{3+} f → f excitation lines [13]. Unfortunately, sensitization of Eu^{3+} by Ce^{3+} is hampered by metal-to-metal charge transfer (MMCT) quenching $Ce^{3+}/Eu^{3+} \leftrightarrow Ce^{4+}/Eu^{2+}$ which leads to a low quantum efficiency of such phosphors [14]. The $Ce^{3+} \rightarrow Eu^{3+}$ energy transfer (ET) is restricted to distances of less than 6 Å, whereas MMCT can take place over ranges of as much as 12–14 Å [15,16]. It follows that it is impossible to achieve direct ET between Ce^{3+} and Eu^{3+} without simultaneous MMCT quenching. Nevertheless, Blasse et al. showed that ET between Ce^{3+} and Eu^{3+} is possible if sensitizer and activator

---

* Corresponding authors.
E-mail addresses: stefan-fischer@fh-muenster.de (S. Fischer), tj@fh-muenster.de (T. Jüstel).

https://doi.org/10.1016/j.jlumin.2018.07.001
Received 23 March 2018; Received in revised form 29 June 2018; Accepted 1 July 2018

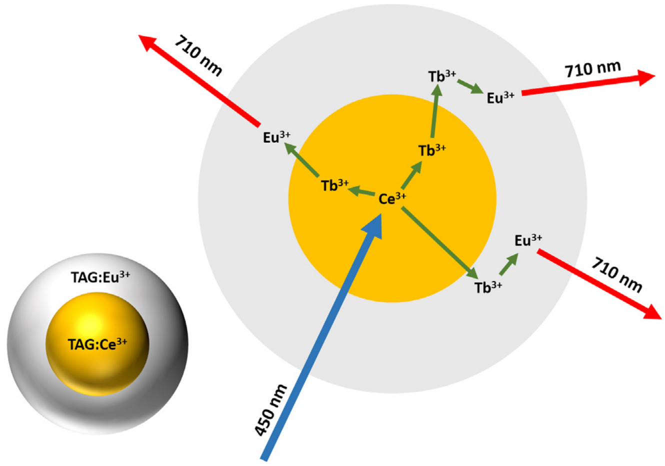

Fig. 1. Schematic structure of core-shell particles (left sketch) and illustration of the luminescence process for converting blue into red light (right sketch).

concentrations are low and Gd^{3+} is used as an intermediate leading to a $Ce^{3+} \rightarrow (Gd^{3+})_n \rightarrow Eu^{3+}$ ET scheme [10]. Furthermore, Setlur demonstrated that Tb^{3+} could also be used as such an intermediate ion [16]. The indirect $Ce^{3+} \rightarrow (Tb^{3+})_n \rightarrow Eu^{3+}$ ET with $n \approx 10^4$ has a far greater range because of energy migration via the Tb^{3+} sublattice [17]. In general, $Ce^{3+} \rightarrow Tb^{3+}$ and $Tb^{3+} \rightarrow Eu^{3+}$ transfer processes are well investigated and occur with rather high energy transfer rates and efficiencies [18,19]. Therefore, Ce^{3+} and Eu^{3+} can be separated sufficiently to prevent MMCT quenching, while still maintaining ET between the two ions via the Tb^{3+} sublattice. One way to realize such spatial separation is to use very low Ce^{3+} and Eu^{3+} concentrations [18]. However, this approach suffers from low emission intensities due to the low activator concentration. Nazarov et al. investigated $Tb_3Al_5O_{12}$:Ce^{3+},Eu^{3+}, were ET between Ce^{3+} and Eu^{3+} is taking place via the Tb^{3+} sublattice, but luminescence is quenched when TAG:Ce^{3+} is co-doped with Eu^{3+} [13].

A more suitable method for spatial separation is the use of core-shell particles. The particles are depicted schematically in Fig. 1. This method has been published by Gui et al. for $NaGdF_4$ [20]. Fluorides offer the advantage that the preparation of core-shell particles is facilitated due to the highly crystalline precipitation of such materials. However, Ce^{3+} shows no absorption in the blue spectral range in fluorides, making this material unsuitable for use as LED phosphor. For that reason, we chose $Tb_3Al_5O_{12}$ (TAG) as the host material, since TAG:Ce^{3+} offers strong absorption around 450 nm, although preparing garnet@garnet core-shell particles appeared to be more demanding than those core-shell particles comprising fluorides. Furthermore, TAG has a high concentration of Tb^{3+} as is required for efficient energy migration via the Tb^{3+} sublattice.

2. Experimental section

2.1. Preparation

The core-shell particles were prepared by homogeneous precipitation using urea as precipitation agent [21]. To investigate ET and MMCT behavior in the core-shell particles, TAG:Ce^{3+} (TC) was coated with TAG:Eu^{3+} (TC@TE) and TAG:Ce^{3+},Eu^{3+} (TC@TCE), respectively. Additionally, non-core-shell particles, viz TAG:Eu^{3+}, which was used to create a blend with TC (TCbTE), and TAG:Ce^{3+},Eu^{3+} (TCE), were prepared by the same synthesis approach without dispersing core material in the mixture. The following synthesis route is suitable for all samples mentioned above. The starting materials Tb_4O_7 (Treibacher Industrie AG, 99.99%), Eu_2O_3 (Treibacher Industrie AG, 99.99%), $Ce(NO_3)_3{\cdot}6H_2O$ (Alfar Aesar, 99.5%) and $Al(NO_3)_3{\cdot}9H_2O$ (VWR Chemicals, 99.6%) were weighed in stoichiometric amounts. The Ce^{3+} and Eu^{3+} contents were set to 3 and 10 mol-%, respectively, since TC has a rather high emission intensity with a Ce^{3+} concentration around 3% and the self-quenching is already taking place at Eu^{3+} concentrations around 10%, which can be observed in TCE. Urea (Merck KGaA, 99.5%) was weighed in a molar ratio of 15:1 relative to the amount of metal cations. The oxides were dissolved in diluted nitric acid, the nitrates and urea in deionized water and the resulting solutions were mixed in a round-bottom flask. 4 g of the TC particles (Litec-LLL GmbH, Greifswald, Germany) have been dispersed in the abovementioned mixture. The amount of shell material was calculated as follows: TC particle size is around 25 µm. The desired thickness of the TE shell was arbitrary set to 3 µm. Using the formula for the volume of a sphere and the density of $Tb_3Al_5O_{12}$, the required shell mass was determined to be around 90% of the core mass. The solution was heated to 90 °C under vigorous stirring and reflux in order to decompose the dissolved urea into CO_2 and NH_3, which increases the pH value and thus the OH^- concentration. The OH^- ions act as a precipitant. After 18 h, the solid phase was separated from the liquid phase by vacuum filtration. Subsequently, the filter cake was dried at 150 °C and the dried material was annealed at 1500 °C in a muffle furnace for 8 h in reducing CO atmosphere.

2.2. Measurements

Phase purity of the prepared samples was determined by powder X-ray diffraction (XRD). The XRD patterns were recorded on a Rigaku MiniFlex II diffractometer working in Bragg-Brentano geometry using Cu Kα radiation.

The photoluminescence (PL) spectra were recorded on an Edinburgh Instruments FLS920 spectrometer equipped with a xenon arc lamp (450 W) and a cooled (−20 °C) single-photon counting photomultiplier (Hamamatsu R2658P). The emission spectra were corrected by applying a correction file obtained from a tungsten incandescent lamp certified by the National Physical Laboratory, UK.

The diffuse reflectance (DR) spectra were recorded on an Edinburgh Instruments FS920 spectrometer equipped with a xenon arc lamp (450 W), a cooled (−20 °C) single-photon counting photomultiplier (Hamamatsu R928) and an integration sphere made of PTFE. $BaSO_4$ (99.99%, Sigma Aldrich) was used as a reflectance standard.

For fluorescence lifetime measurements, a blue laser (Edinburgh Instruments EPL445, 445 nm) was used. Pulse frequency was set to 0.1 MHz. Recorded decay curves were fitted as follows:

$$I = A_1 e^{\frac{-t}{\tau_1}} + A_2 e^{\frac{-t}{\tau_2}} + A_n e^{\frac{-t}{\tau_n}} \tag{1}$$

I is the PL intensity at the time t, A_1 and A_2 are fitting parameters and τ_1 and τ_2 are the partial fluorescence lifetimes of the exponential components. Eq. (1) can be expanded with an arbitrary number of further $A_n e^{\frac{-t}{\tau_n}}$, if a higher exponential fitting is necessary. Average fluorescence lifetimes τ were obtained by applying Eq. (2):

$$\tau = \frac{A_1 \tau_1^2 + A_2 \tau_2^2}{A_1 \tau_1 + A_2 \tau_2} \tag{2}$$

The temperature dependent PL spectra from 77 to 500 K were recorded using an Oxford Instruments cryostat MircostatN2. Liquid nitrogen was used as cooling agent. Temperature stabilization time amounted to 30 s and tolerance was set to ± 3 K.

External quantum efficiencies (EQE) were calculated using the approach of Kawamura et al. [22], which describes the absolute ratio between emitted and absorbed photons of a specific wavelength. The emission spectra of $BaSO_4$ (99.99%, Sigma Aldrich) and of the investigated samples were measured in an integration sphere made of PTFE.

The scanning electron microscopy (SEM) images were taken on a Zeiss EVO MA10 using a secondary electron detector and operating in